Effects of nonpolar solutes on the thermodynamic response functions of aqueous mixtures

Swaroop Chatterjee
Department of Chemical Engineering, Princeton University, Princeton, New Jersey 08544

Henry S. Ashbaugh
Department of Chemical and Biomolecular Engineering, Tulane University, New Orleans, Louisiana 70118

Pablo G. Debenedetti[a)]
Department of Chemical Engineering, Princeton University, Princeton, New Jersey 08544

(Received 8 July 2005; accepted 24 August 2005; published online 21 October 2005)

We investigate the effect of adding nonpolar solutes at atmospheric pressure on water's temperature of maximum density, isothermal compressibility, and isobaric heat capacity, using a statistical mechanical model of water solutions [H. S. Ashbaugh, T. M. Truskett, and P. G. Debenedetti, J. Chem. Phys. **116**, 2907 (2002)]. We find that the temperature of maximum density increases with solute hydrophobicity, as characterized by its size, and decreases with its van der Waals attractive parameter a, in agreement with experiment. We predict similar trends for the addition of solutes on the isothermal compressibility and isobaric heat capacity: solute hydrophobicity causes an upward shift in water's anomalies, whereas dispersive interactions as measured by the solute's van der Waals attractive parameter shift the anomalies to lower temperatures. The locus along which the competing contributions of solute size σ and interaction strength a to the shift in water's response functions balance each other obeys the scaling relationship $\sigma^6 \sim a$. © *2005 American Institute of Physics*. [DOI: 10.1063/1.2075127]

I. INTRODUCTION

Aqueous solutions of nonpolar species are a subject of considerable scientific interest, in no small measure on account of the central role that hydrophobic hydration is believed to play in biological self-assembly phenomena.[1–3] Recent theoretical work has linked many of the distinctive features of hydrophobic hydration, such as the minimum with respect to temperature in the solubility of nonpolar solutes (believed to play a role in the cold denaturation of proteins), to the temperature of maximum density (T_{MD}) of pure liquid water at 4 °C.[4–13] It is therefore of interest to investigate the effect of added solutes on the T_{MD}. More generally, a systematic understanding of the effects of solutes on water's thermodynamic anomalies, such as the pronounced increase of the isobaric heat capacity and the isothermal compressibility upon cooling,[14] is of relevance to atmospheric physics,[15,16] plant physiology,[17] water pollution,[18] and self-assembly.[1–3] In this paper we investigate theoretically the effect of nonpolar solutes on water's response functions (coefficient of thermal expansion, isobaric heat capacity, and isothermal compressibility) using a simple statistical mechanical theory of water[19] and of its mixtures with nonpolar solutes.[4] This theory has been shown to reproduce water's equation-of-state anomalies[19] and the thermodynamic signatures of hydrophobic hydration.[4]

To illustrate the subtleties of the phenomena under investigation, consider a dilute mixture of a solute (s) in water (w). For isobaric changes in temperature in the vicinity of pure water's temperature of maximum density (T^0_{MD}), the partial molar volumes can be written as

$$\bar{v}_w(T) = \bar{v}_w(T^0_{\mathrm{MD}}) + \frac{\lambda}{2}(T - T^0_{\mathrm{MD}})^2, \tag{1}$$

$$\bar{v}_s(T) = \bar{v}_s(T^0_{\mathrm{MD}}) + \chi(T - T^0_{\mathrm{MD}}), \tag{2}$$

where $\lambda > 0$ (the volume is a minimum at the T_{MD} with respect to isobaric temperature changes). The temperature dependence of the mixture's molar volume at fixed pressure and composition is given by

$$\left(\frac{\partial v}{\partial T}\right)_{P,x_s} = x_w\lambda(T - T^0_{\mathrm{MD}}) + x_s\chi, \tag{3}$$

where x_w and x_s are the water and solute mole fractions, respectively. Setting the derivative to zero, solving for T and differentiating with respect to x_s, we obtain, in the limit of infinite dilution, the relationship

$$\left(\frac{\partial T_{\mathrm{MD}}}{\partial x_s}\right)^{\infty}_{P} = -\frac{\chi}{\lambda}. \tag{4}$$

Thus, if the solute's partial molar volume increases with temperature ($\chi > 0$, the usual situation), we expect the T_{MD} of the mixture to shift to lower temperatures and ultimately be occluded by the solution's freezing point. Ionic solutes as well as a number of hydrophilic species indeed suppress the T_{MD} of water.[20–26] However, systematic studies of homologous series of soluble species containing hydrophobic units, such

[a)]Electronic mail: pdebene@princeton.edu

as the *n*-alkyl alcohols, have shown that nonpolar groups can actually shift the T_{MD} above that of pure water.[27–31] This surprising result has been ascribed to the tendency of hydrophobic moieties to locally enhance the hydrogen-bond network in water, and hence to shift water's anomalies to higher temperatures. In terms of the above analysis, the positive shift of the T_{MD} implies that the solute's partial molar volume at infinite dilution decreases with increasing temperature. This is consistent with the notion of an open water structure around hydrophobic solutes progressively disrupted by thermal motion. Though plausible, such interpretations of T_{MD} shifts are largely qualitative. Microscopic models have yet to be applied to the problem of understanding the effects of solutes on water's response functions. The purpose of this work is to begin to fill this gap in understanding.

Recently we developed a statistical mechanical model of liquid water[19] and of its mixtures with van der Waals solutes.[4] Here we use this model to study the effects of nonpolar solutes on water's T_{MD}, isothermal compressibility, and isobaric heat capacity.[32–37] In particular, we make specific predictions on the effects of solute size and solute-solvent dispersion forces on water's response functions. The paper is organized as follows. In Sec. II we summarize the statistical mechanical model. Sec. III presents the results on the effect of solute addition upon the T_{MD}. The corresponding effects on the compressibility and heat-capacity anomalies are discussed in Sec. IV. We summarize the main conclusions and suggest directions for future research in Sec. V.

II. STATISTICAL MECHANICAL MODEL

Previously, we developed an analytical statistical thermodynamic framework for describing the anomalous properties of liquid water[19] and aqueous mixtures with a van der Waals fluid.[4] Here we summarize the key equations for aqueous solutions and provide only a brief description. A detailed derivation and discussion is presented in Refs. 4 and 19

In the present model, the canonical partition function of a mixture of N_w water molecules and N_s solute molecules in a volume V at temperature T is written as

$$Q(N_w,N_s,V,T)=\left(\frac{1}{N_w!N_s!\Lambda_w^{3N_w}\Lambda_s^{3N_s}}\right)(V-Nb)^N \times\exp(N\beta\rho a)(4\pi)^{N_w}\prod_{j=1}^{j_{\max}}\prod_{k=0}^{k_{\max}} f_{j,k}^{N_w p_{j,k}}. \quad (5)$$

In this expression Λ_i is the thermal wavelength of component i, $N=N_w+N_s$ is the total number of molecules, and $\beta^{-1}=k_BT$ is the product of Boltzmann's constant and the temperature. a and b are the familiar van der Waals attractive interaction and excluded volume parameters for the mixture. Standard mixing rules were applied to evaluate the solution a and b parameters,

$$a=x_w^2a_{ww}+2x_wx_sa_{sw}+x_s^2a_{ss}, \quad (6a)$$

$$b=x_wb_w+x_sb_s, \quad (6b)$$

where $x_i=N_i/N$ is the mole fraction of component i, and the cross solute-water van der Waals interaction parameter is given by $a_{sw}=\sqrt{a_{ww}a_{ss}}$. The pure component excluded volume parameters are determined by the individual component van der Waals diameters, σ_i, so that the pressure diverges at the random close packing density

$$0.64b_i=\frac{\pi\sigma_i^3}{6}, \quad (7)$$

where the spheres occupy 64% of the volume.

The first three terms in the product on the right side of Eq. (5) comprise the partition function of a van der Waals mixture. The last two terms constitute the contribution of aqueous hydrogen bonding. $p_{j,k}$ is the probability that j water molecules and k solute molecules occupy the bonding shell of a central water molecule, while the inner exclusion shell of the central water is devoid of both water and solute molecules (see Fig. 1).[4] We assumed previously,[4] and here, that the solute-mediated effect on water hydrogen bonding is zero. Different choices (e.g., solute-induced hydrogen-bond weakening, hydrogen-bond enhancement) can easily be incorporated into the calculations, although we have not done so here. $f_{j,k}$ arises from orientational contributions to the hydrogen-bonding partition function for a central molecule with j water molecules and k solute molecules in its bonding shells and is given by

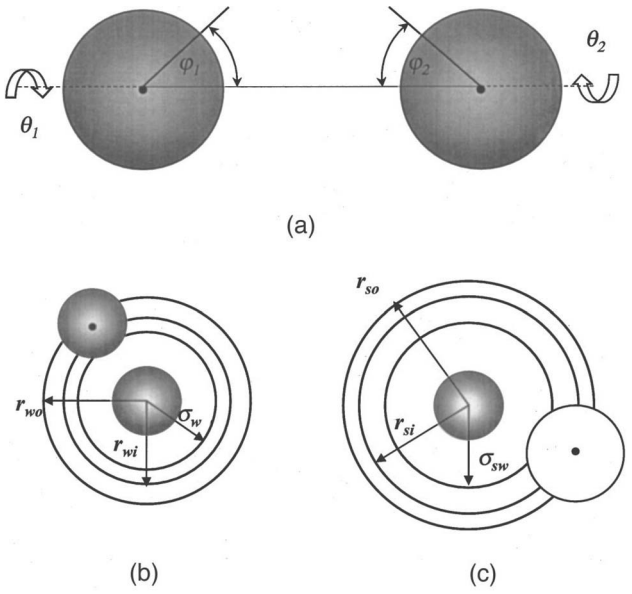

FIG. 1. Representation of the hydrophobic hydration model (Ref. 4). (a) In order to form a hydrogen bond, two water molecules must be properly oriented ($\varphi_1,\varphi_2<\varphi^*$) regardless of the value of θ_1 and θ_2. (b) Water molecules have a hard core of radius σ_w, within which the center of no other molecule can penetrate. To form a hydrogen bond, a central water molecule must be surrounded by an exclusion shell of radius r_{wi}, devoid of centers of other water molecules, and a properly oriented second water molecule must be within its hydrogen bonding shell ($r_{wi}\leqslant r\leqslant r_{wo}$). The presence of additional crowding water molecules within the hydrogen bonding shell weakens an existing bond. (c) Water molecules (gray) have a hard-core radius $\sigma_{sw}=(\sigma_w+\sigma_s)/2$, within which the center of no other solute (white) can penetrate. In order to form a hydrogen bond a central water molecule must also be surrounded by a solute exclusion shell of radius r_{si}. Solutes whose centers are in the hydration shell ($r_{si}\leqslant r\leqslant r_{so}$) can affect the strength of a hydrogen bond (Ref. 4).

TABLE I. Water parameters for single bond model (Ref. 4).

σ_w	3.135 Å
r_{wi}	$1.008\sigma_w$
r_{wo}	$1.04\sigma_w$
a_{ww}	0.310 Pa $\mathrm{m}^6/\mathrm{mol}^2$
ϕ^*	0.175 rad
$\epsilon_{\max}$	23 kJ/mol
ϵ_{pen}	3 kJ/mol
$j_{\max}$	8

$$f_{j,k}=\left[1+\frac{j}{4}(1-\cos\phi^*)^2(e^{\beta\epsilon_{j,k}}-1)\right], \tag{8}$$

where ϕ^* is the critical angle for water hydrogen bonding, and $\epsilon_{j,k}$ is the hydrogen-bonding energy between a pair of water molecules when there are $(j-1)$ crowding water molecules and k solute molecules in the central bonding shell.

$$-\epsilon_{j,k}=-\epsilon_{\max}+(j-1)\epsilon_{\mathrm{pen}}+k\epsilon_{\mathrm{np}}. \tag{9}$$

In this expression $\epsilon_{\max}$ is the energy of a solitary water-hydrogen bonding pair, while ϵ_{pen} and ϵ_{np} are the contributions associated with the addition of other water molecules and nonpolar solutes to the bonding and hydration shell, respectively.

The thermodynamic properties of aqueous mixtures can be determined by appropriate manipulations of the partition function. Of central interest to the present study is the mixture equation of state (EOS), which is given by the volume derivative of the Helmholtz free energy,

$$P=\frac{\rho k_B T}{1-\rho b}-a\rho^2+N_w k_B T\sum_{j=1}^{j_{\max}}\sum_{k=0}^{k_{\max}}\left(\frac{\partial p_{j,k}}{\partial V}\right)_{T,N_w,N_s}\ln f_{j,k}, \tag{10}$$

where $\rho=\rho_s+\rho_w$, the total number density, is the sum of the water and solute number densities. In the limits $\rho_w\to 0$ and $\rho_s\to 0$, the above equation reduces to the van der Waals EOS or to the EOS of pure water,[19] respectively. To determine the densities of water and its mixtures, the system volume is varied at fixed N_w, N_s, and T until the target pressure (1 atm throughout this work) is obtained. We have previously determined a set of parameters for the EOS that accurately captures the properties of water at atmospheric pressure and produces a density maximum at 4.14 °C. The parameter set used here for aqueous solutions is given in Table I. In what follows, we examine the effects of solute size and attractive interactions on the T_{MD}, compressibility, and heat capacity of aqueous mixtures.

III. EFFECT OF SOLUTES ON THE T_{MD}

Figure 2 shows experimental data on the effect of different solutes upon the T_{MD} of aqueous mixtures at atmospheric pressure. It can be seen that some solutes, such as propylene glycol, and ethylene glycol, cause a monotonic decrease in the T_{MD}, while the addition of other solutes such as methyl alcohol, ethyl alcohol, and *t*-butyl alcohol causes the T_{MD} to increase above the pure water value at low solute mole fractions. For these solutes the T_{MD} eventually reaches a maximum with respect to solute mole fraction, and decreases monotonically upon further solute addition. According to Wada and Umeda,[27] increases in the T_{MD} upon solute addition are a consequence of solute-solute interactions that are weak relative to solute-solvent interactions. Figure 3 shows the theoretical predictions of the composition dependence of the mixture T_{MD} at atmospheric pressure for aqueous solutions of methyl alcohol and of ethyl alcohol according to the hydrophobic hydration model of Ashbaugh *et al.*[4] The van der Waals parameters for the solutes were computed from experimental values of critical temperature and pressure using the relations

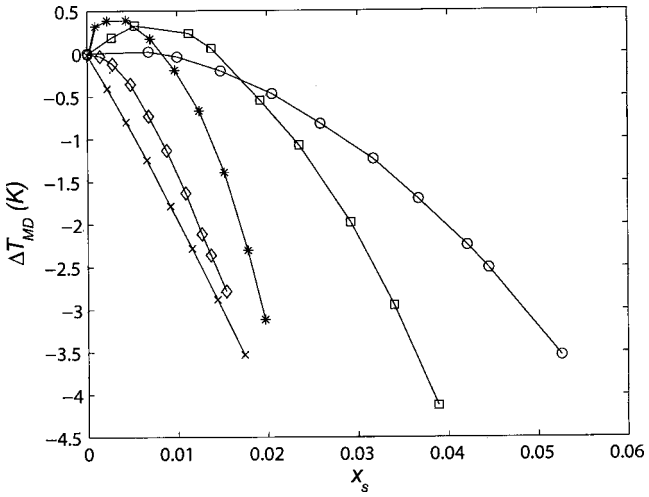

FIG. 2. Change in T_{MD} at atmospheric pressure with solute mole fraction for five solutes: methyl alcohol (○), ethyl alcohol (□), *t*-butyl alcohol (∗), propylene glycol (◇), and ethylene glycol (×) (Experimental data from Ref. 27).

$$a_{\mathrm{ss}}=\frac{27k_B^2T_c^2}{64P_c}, \tag{11}$$

$$b_s=\frac{k_BT_c}{8P_c}. \tag{12}$$

The water parameters are given in Table I. It can be seen that the model is able to capture qualitatively the experimental

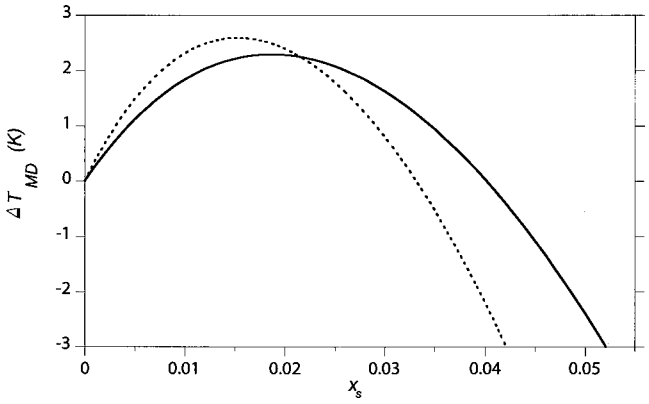

FIG. 3. Predicted T_{MD} shifts for methanol (solid line) and ethanol (dashed line) from the hydrophobic hydration model (Ref. 4) using van der Waals parameters fit to critical properties of the alcohols (MeOH-σ_s=5.144 Å and a_{ss}=0.966 Pa m^6 mol^{-2}; EtOH-σ_s=5.546 Å and a_{ss}=1.218 Pa m^6 mol^{-2}).

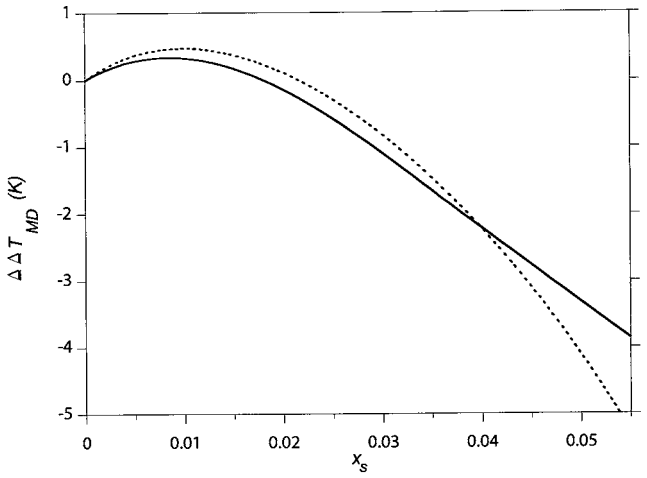

FIG. 4. Difference in the T_{MD} shifts for ethanol and methanol, $\Delta\Delta T_{MD} = \Delta T_{MD}(\text{EtOH}) - \Delta T_{MD}(\text{MeOH})$. The solid line represents theoretical prediction; dashed line, experiment (Ref. 27).

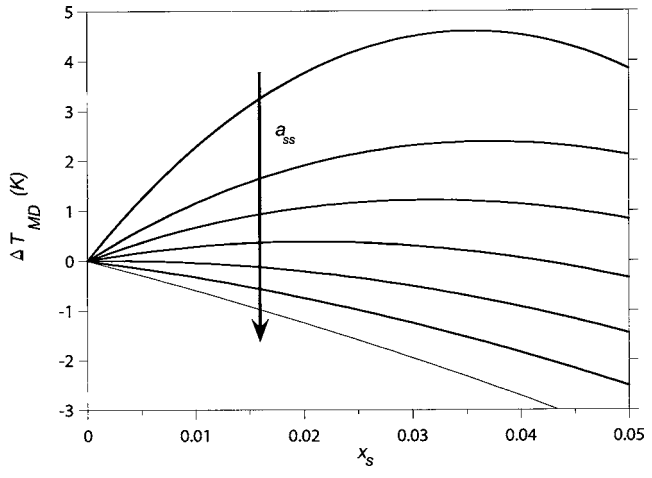

FIG. 6. Shift in T_{MD} at atmospheric pressure with increasing strength of solute-solute interactions for a solute of fixed size $\sigma_s = 4$ Å. The top curve corresponds to $a_{ss}=0$, while subsequent curves represent the effect of increasing a_{ss} in the direction of the arrow in increments of 0.2 Pa m^6 mol^{-2}.

observations (see Fig. 2). Both T_{MD} curves exhibit a maximum, whose value is greater for ethyl alcohol than for methanol. The numerical values of the T_{MD}, however, do not agree well with experimental behavior. One reason for this discrepancy is the fact that the hydrophobic hydration model considers solutes to be spherical. The nonspherical shape of the alcohol molecules and the hydrogen bonding between the solutes and water are not included in this analysis. One way to compensate for these model limitations is to consider the incremental effect of one methylene group $\Delta\Delta T_{MD} = \Delta T_{MD}(\text{EtOH}) - \Delta T_{MD}(\text{MeOH})$. Figure 4 shows that the model predictions for this incremental effect are in good agreement with experiment.[27] Therefore, even though the mixture equation of state is unable to describe the effect of hydrogen bonding between solute and solvent molecules, or accurately account for the geometry of the solute, it captures the incremental effect of increasing solute hydrophobicity on the T_{MD}.

Figure 5 shows the calculated locus in the (a_{ss}, σ_s) plane at atmospheric pressure separating solutes that, like methanol, ethanol, and *t*-butanol, cause a positive shift in the T_{MD}, from those, such as ethylene glycol and propylene glycol, that cause a negative shift. It can be seen that solute size and

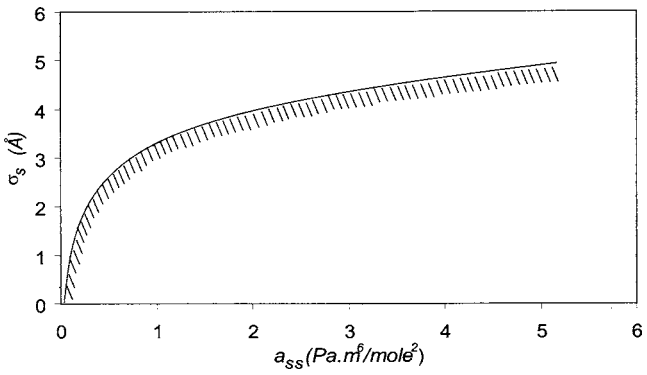

FIG. 5. Effect of solute characteristic size and energy parameters, σ_s and a_{ss}, at atmospheric pressure on the temperature of maximum density (T_{MD}). On the shaded side of the curve, the T_{MD} decreases upon solute addition. Model parameters for water are given in Table I obtained from Ref. 4.

solute-solute interactions have opposite effects on the T_{MD}: increasing the former causes $\partial T_{MD}/\partial x_s$ at infinite dilution to increase whereas strong solute-solute attractions cause $\partial T_{MD}/\partial x_s$ at infinite dilution to decrease. The effect of solute-solute attractions is illustrated in Fig. 6, where the calculated T_{MD} shifts for a 4 Å solute at atmospheric pressure are shown for increasing values of a_{ss} (top to bottom). The calculations explain the observation of Wada and Umeda[27] that weak solute-solute interactions relative to solute-solvent interactions cause the T_{MD} to shift to higher temperatures upon solute addition. In our model $a_{ss}/a_{sw} = (a_{ss}/a_{ww})^{1/2}$, so decreasing a_{ss} at fixed a_{ww} is equivalent to weakening solute-solute interactions relative to solute-solvent interactions.

It is possible to derive an analytical expression for the curve shown in Fig. 5. To this end, we write the identity

$$\left.\frac{\partial T_{MD}}{\partial x_s}\right|_P^\infty = \rho_w \bar{v}_s^\infty \left.\frac{\partial T_{MD}}{\partial \phi_s}\right|_P^\infty, \tag{13}$$

where the superscript ∞ denotes infinite dilution, $\bar{v}_s^\infty$ is the solute partial molar volume at infinite dilution, ρ_w is the number density of water molecules, and ϕ_s is the solute volume fraction ($\phi_s = x_s \bar{v}_s / v = \rho_s \bar{v}_s$). Figure 7 shows the volume fraction dependence of the T_{MD} for hard-sphere solutes of varying sizes. It can be seen that the limiting slope of the T_{MD} vs ϕ_s curves is essentially independent of solute size. Hence, for hard-sphere solutes, $(\partial T_{MD}/\partial x_s)_P^\infty$ should be directly proportional to the solute's partial molar volume. This expectation is borne out when $(\partial T_{MD}/\partial x_s)_P^\infty$ is plotted as a function of $\bar{v}_s^\infty$ (see Fig. 8).

Next, we write the thermodynamic identity (see Appendix for derivation)

$$\left(\frac{\partial T_{MD}}{\partial x_s}\right)_P^\infty = \rho_w^2 \bar{v}_s^\infty \frac{(\partial^2 P/\partial T \partial \rho_w)^0}{(\partial^2 P/\partial T^2)_\rho^0} - \frac{(\partial^2 P/\partial T \partial x_s)^\infty}{(\partial^2 P/\partial T^2)_\rho^0}, \tag{14}$$

where the superscript ∞ denotes an infinite dilution quantity, and the superscript 0 denotes a pure solvent quantity. The distinction between infinite dilution and pure solvent quantities is that the latter do not depend on any solute characteristics (e.g., σ_s), whereas the former do. It is shown in the

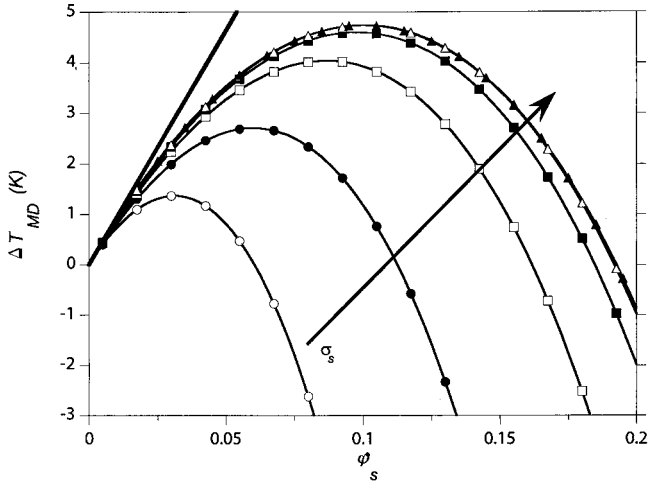

FIG. 7. Shift in atmospheric pressure T_{MD} for hard-sphere solutes of different sizes (size increasing from 1 to 6 Å in the direction of the arrow), as a function of solute volume fraction. The limiting tangent has a slope $(\partial T_{\mathrm{MD}}/\partial \phi_s)_P^{\infty}=92.4$ K.

Appendix that for the EOS considered here, every second derivative of the pressure in Eq. (14) is independent of a_{ss}. Hence the difference between the T_{MD} shift [left-hand side of Eq. (14)] due to a solute with nonzero van der Waals attractive parameter and the T_{MD} shift due to a hard-sphere solute of the same size is given by

$$\left(\frac{\partial T_{\mathrm{MD}}}{\partial x_s}\right)_{P,a_{\mathrm{ss}}\neq 0}^{\infty}-\left(\frac{\partial T_{\mathrm{MD}}}{\partial x_s}\right)_{P,a_{\mathrm{ss}}=0}^{\infty}=\rho_w^2\frac{(\partial^2 P/\partial T\partial\rho_w)^0}{(\partial^2 P/\partial T^2)_\rho^0}[\bar{v}_s^{\infty}(\sigma_s,a_{\mathrm{ss}}\neq 0)-\bar{v}_s^{\infty}(\sigma_s,a_{\mathrm{ss}}=0)]. \quad (15)$$

As shown in the Appendix,

$$\bar{v}_s^{\infty}(\sigma_s,a_{\mathrm{ss}}\neq 0)-\bar{v}_s^{\infty}(\sigma_s,a_{\mathrm{ss}}=0)=-2K_T^0\rho_w a_{\mathrm{sw}}. \quad (16)$$

It follows from Eqs. (13), (15), and (16) that

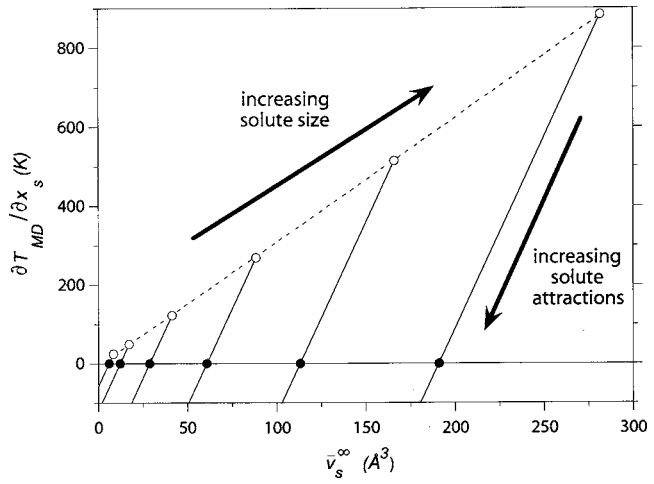

FIG. 8. Slope of the atmospheric pressure T_{MD} upon solute addition at infinite dilution ($\partial T_{\mathrm{MD}}/\partial x_s|_P^{\infty}$) as a function of the solute's partial molar volume ($\bar{v}_s^{\infty}$). The dashed line corresponds to the prediction for hard-sphere solutes. The open points are the results for different solute sizes (from 1 to 6 Å). The filled points indicate the condition when the T_{MD} shift is zero.

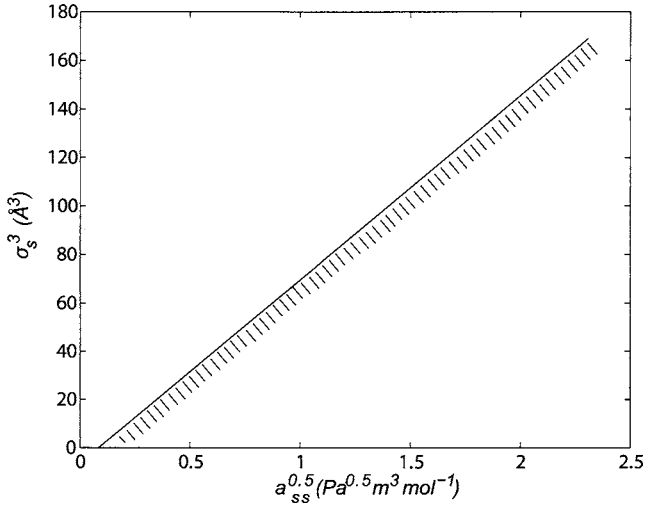

FIG. 9. Correlation between solute size and attractive interactions for $\partial T_{\mathrm{MD}}/\partial x_s|_P^{\infty}=0$. Here, σ_s^3 is plotted vs $a_{\mathrm{ss}}^{0.5}$. In the shaded region, $\partial T_{\mathrm{MD}}/\partial x_s|_P^{\infty}<0$, whereas $\partial T_{\mathrm{MD}}/\partial x_s|_P^{\infty}>0$ above the line.

$$\left(\frac{\partial T_{\mathrm{MD}}}{\partial x_s}\right)_{P,a_{\mathrm{ss}}\neq 0}^{\infty}=\rho_w\bar{v}_s^{\infty}(a_{\mathrm{ss}}=0)\left(\frac{\partial T_{\mathrm{MD}}}{\partial \phi_s}\right)_P^{\infty}-2K_T^0 a_{\mathrm{sw}}\rho_w^3\frac{(\partial^2 P/\partial T\partial\rho_w)^0}{(\partial^2 P/\partial T^2)_\rho^0}. \quad (17)$$

Hence, the line in $(\sigma_s,a_{\mathrm{ss}})$ parameter space along which $(\partial T_{\mathrm{MD}}/\partial x_s)_P^{\infty}$ vanishes must satisfy

$$\bar{v}_s^{\infty}(a_{\mathrm{ss}}=0)=\left[\frac{2K_T^0\rho_w^2(\partial^2 P/\partial T\partial\rho_w)^0\sqrt{a_{\mathrm{ww}}}}{(\partial^2 P/\partial T^2)_\rho^0(\partial T_{\mathrm{MD}}/\partial\phi_s)_P^{\infty}}\right]a_{\mathrm{ss}}^{1/2}\equiv\gamma a_{\mathrm{ss}}^{1/2}, \quad (18)$$

where γ is a water-specific quantity that depends on P and T only, and we have used [both in Eq. (18) and throughout this work] the combining rule $a_{\mathrm{sw}}=(a_{\mathrm{ww}}a_{\mathrm{ss}})^{1/2}$. If, furthermore, we assume $\bar{v}_s^{\infty}\propto\sigma_s^3$, we obtain, finally,

$$\sigma_s^3\propto a_{\mathrm{ss}}^{1/2}. \quad (19)$$

Because point solutes have nonvanishing partial molar solutes (see Appendix), one expects in general $\bar{v}_s^{\infty}(a_{\mathrm{ss}}=0)=m\sigma^3+q$. It is therefore of interest to check the validity of Eq. (19). Figure 9 shows that, indeed, there is a linear correlation between $a_{\mathrm{ss}}^{1/2}$ and σ_s^3 when the full model is used to calculate the value of a_{ss} that causes $(\partial T_{\mathrm{MD}}/\partial x_s)_P^{\infty}$ to vanish, for any given value of σ_s. The y intercept of this correlation, however, is not zero, since the assumption that $(\partial T_{\mathrm{MD}}/\partial x_s)_P^{\infty}$ is independent of solute size breaks down for small solutes (see Fig. 7). Nevertheless, the reasoning underlying the correlation of Fig. 9 provides insight into the balance between the hydrophilic and hydrophobic characteristics of a solute, as embodied in a_{ss} and σ_s, which shift the T_{MD} of aqueous solutions.

IV. EFFECT OF SOLUTES ON COMPRESSIBILITY AND HEAT-CAPACITY ANOMALIES

We also investigated the effect of adding nonpolar solutes on water's isothermal compressibility and isobaric heat capacity. At atmospheric pressure, the former quantity exhib-

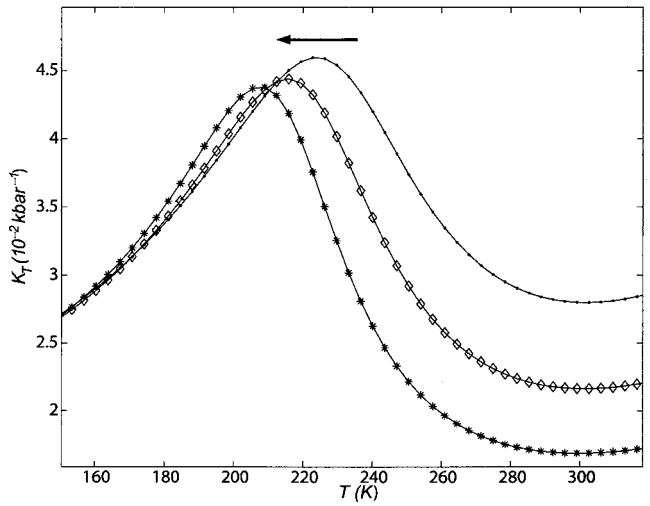

FIG. 10. Temperature dependence of the isothermal compressibility (K_T) at atmospheric pressure. Aqueous solution of van der Waals solute (a_{ss} =2 Pa m^6/mol^2, σ_s=2 Å) shows a shift of the temperature of the metastable maximum in K_T to lower temperature due to solute addition. The arrow indicates the direction of increasing mole fraction of solute (x_s=0.001, ●; x_s=0.005, ◇; x_s=0.01, ∗).

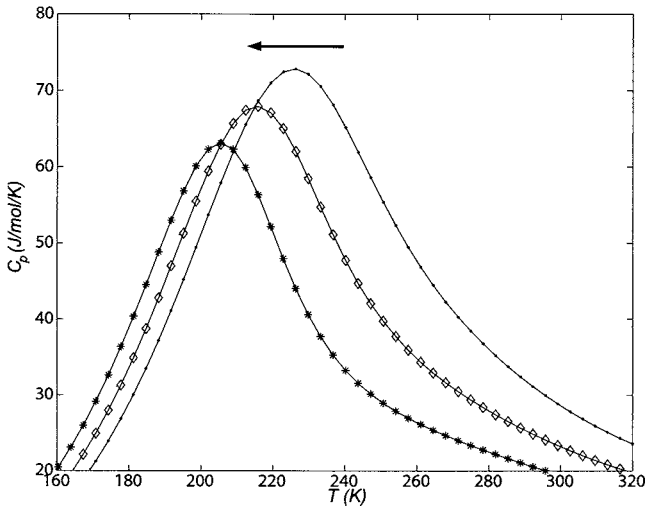

FIG. 11. Temperature dependence of the isobaric heat capacity (C_p) at atmospheric pressure. Aqueous solution of van der Waals solute (a_{ss} =2 Pa m^6/mol^2, σ_s=2 Å) shows a shift of the temperature of the metastable maximum in C_p to lower temperature due to solute addition. The arrow indicates the direction of increasing mole fraction of solute (x_s=10^{-16}, ●; x_s=0.01, ◇; x_s=0.02, ∗).

its a broad minimum with respect to temperature at 46 °C, below which temperature the compressibility increases sharply upon cooling.[14] Experimentally, it is found that the anomalous increase in compressibility upon cooling continues down to the homogeneous nucleation temperature. The isobaric heat capacity likewise exhibits a broad atmospheric pressure minimum with respect to temperature at 33 °C, below which temperature it increases sharply upon cooling down to the homogeneous nucleation temperature.[14]

Both the compressibility and the heat capacity can be readily calculated from the hydrophobic hydration model by differentiation of the equation of state and the partition function, respectively.[4] It was found that the temperatures at which the compressibility and heat capacity exhibit minima are rather insensitive to the mixture's composition for the dilute conditions considered here (Figs. 10 and 11). In contrast, the low-temperature maxima for both response functions are predicted to be sensitive functions of composition (Figs. 10 and 11). Accordingly, the atmospheric pressure maxima with respect to temperature of both the compressibility and heat capacity were used as indicators of the effect of solute addition. For solutes that enhance water's anomalies one expects to see the maxima shift to higher temperatures; vice versa, for solutes that suppress water's anomalies, the maxima in heat capacity and compressibility are expected to shift to lower temperatures upon solute addition.

Figure 12 shows the calculated boundary in the (a_{ss}, σ_s) plane, separating solutes that shift the compressibility and heat-capacity maxima to lower-temperature (suppression of anomalies: high a_{ss}, low σ_s region) from solutes that shift the anomalies to higher temperatures (enhancement of anomalies: low a_{ss}, high σ_s region), at atmospheric pressure. It can be seen that both loci coincide in the limit of small a_{ss} and σ_s. Interestingly, we find that the isothermal compressibility and T_{MD} loci coincide over the entire range of parameters explored here.

The overall picture that emerges from Fig. 12 is as follows: solute-solute attractions and hence (by the Lorentz-Berthelot mixing rules adopted here) solute-solvent attractions suppress water's anomalies, and shift the compressibility and heat-capacity maxima as well as the T_{MD} towards lower temperatures. Hard-sphere solutes enhance water's anomalies, shifting the compressibility and heat-capacity maxima as well as the T_{MD} towards higher temperatures. This effect is more pronounced the larger the solute.

V. CONCLUSIONS

In this work we have applied a statistical mechanical model of water solutions to investigate the effects of nonpolar solutes on the T_{MD}, isobaric heat capacity, and isothermal compressibility at atmospheric pressure. The model reproduces the experimentally observed differential shift in the T_{MD} for *n*-alkyl alcohols, and thereby provides a useful framework for interpreting solute effects on the T_{MD}. In par-

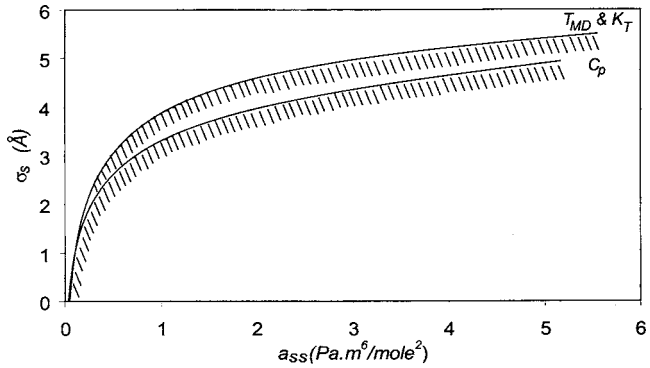

FIG. 12. Effect of solute molecule diameter σ_s and a_{ss} at atmospheric pressure on temperature of maximum density (T_{MD}), isobaric heat capacity (C_p), and isothermal compressibility (K_T). Shading is used to indicate regions of "normal" response function behavior. Model parameters for water are given in Table I obtained from Ref. 4.

ticular, we find that the T_{MD} is shifted to higher temperatures, at infinite dilution, with increasing solute hydrophobicity, as characterized by its van der Waals radius. The T_{MD} is shifted to lower temperatures with increasing solute-solvent attractions. These predictions are in agreement with observed experimental trends.[27] For simple van der Waals solutes we derived a scaling relationship between solute size (σ) and interaction strength (a) such that these competing contributions to the T_{MD} shift balance each other. This scaling relationship is of the form $\sigma^6 \sim a$.

By studying numerically the effect of solute addition on the low-temperature maxima in the isobaric heat capacity and the isothermal compressibility we found very similar trends, namely, that increased solute hydrophobicity causes an upward temperature shift in water's anomalies, and conversely increased dispersive attractions among solute molecules cause the anomalies to move to lower temperatures. The (σ,a) locus along which these competing effects on a given property exactly balance is numerically indistinguishable for the case of T_{MD} and isothermal compressibility. The corresponding heat-capacity curve is very similar but shifted so that smaller solutes (fixed a) can cause a positive temperature shift in the location of heat-capacity maxima than can do so for the T_{MD}. Equivalently, a larger a (fixed σ) is needed to cause a negative shift in the location of the heat-capacity extremum.

Several avenues of future inquiry are suggested by this work. Our analysis has been restricted to atmospheric pressure. Given the sensitive manner in which liquid water's anomalies depend on pressure, it will be interesting to perform analogous calculations over a wide range of pressures. Such calculations are in progress. An important limitation of the statistical mechanical model on which our analysis is based is its neglect of electrostatic forces. These play an important role both in pure water and in its mixtures with ionic solutes. Extension of the model to encompass this important class of systems is another interesting direction for future investigations. Finally, we mention the desirability to generalize the model to nonspherical solutes.

ACKNOWLEDGMENTS

One of the authors (P.G.D.) gratefully acknowledges the support of the National Science Foundation through Collaborative Research in Chemistry Grant No. CHE 0404699. Another author (H.S.A.) is grateful to L. R. Pratt (Los Alamos) for insightful discussions.

APPENDIX: DERIVATIONS

1. Derivation of Eq. (14)

Consider the derivative

$$\left(\frac{\partial P}{\partial T}\right)_{V,N_w,N_s} = \frac{\alpha_p}{K_T} \equiv \psi(T,V,N_w,N_s) \tag{A1}$$

which vanishes at the T_{MD}. In general,

$$d\psi = \left(\frac{\partial \psi}{\partial T}\right)_{V,N_w,N_s} dT + \left(\frac{\partial \psi}{\partial V}\right)_{T,N_w,N_s} dV + \left(\frac{\partial \psi}{\partial N_w}\right)_{V,T,N_s} dN_w + \left(\frac{\partial \psi}{\partial N_s}\right)_{V,T,N_w} dN_s \tag{A2}$$

and, therefore, along a curve of constant ψ,

$$0 = \left(\frac{\partial \psi}{\partial T}\right)_{V,N_w,N_s}\left(\frac{\partial T}{\partial N_s}\right)_{P,N_w,\psi} + \left(\frac{\partial \psi}{\partial V}\right)_{T,N_w,N_s}\left(\frac{\partial V}{\partial N_s}\right)_{P,N_w,\psi} + \left(\frac{\partial \psi}{\partial N_s}\right)_{V,T,N_w}. \tag{A3}$$

Solving for $(\partial T/\partial N_s)_{P,N_w,\psi}$, and multiplying by N_w,

$$N_w\left(\frac{\partial T}{\partial N_s}\right)_{P,N_w,\psi} = -N_w\left(\frac{\partial V}{\partial N_s}\right)_{P,N_w,\psi}\frac{(\partial\psi/\partial V)_{T,N_w,N_s}}{(\partial\psi/\partial T)_{V,N_w,N_s}} - N_w\frac{(\partial\psi/\partial N_s)_{V,T,N_w}}{(\partial\psi/\partial T)_{V,N_w,N_s}}. \tag{A4}$$

Consider first the left-hand side. When $\psi=0$, $T=T_{MD}$, so

$$\lim_{\psi\to 0} N_w\left(\frac{\partial T}{\partial N_s}\right)_{P,N_w,\psi} = N_w\left(\frac{\partial T_{MD}}{\partial N_s}\right)_{P,N_w} = x_w^2\left(\frac{\partial T_{MD}}{\partial x_s}\right)_P. \tag{A5}$$

Therefore at infinite dilution,

$$\lim_{x_s\to 0} N_w\left(\frac{\partial T_{MD}}{\partial N_s}\right)_{P,N_w} = \left(\frac{\partial T_{MD}}{\partial x_s}\right)_P^{\infty}. \tag{A6}$$

We next consider the right-hand side derivative $(\partial V/\partial N_s)_{P,N_w,\psi}$ in (A4). In general,

$$dV = \left(\frac{\partial V}{\partial T}\right)_{P,N_w,N_s} dT + \left(\frac{\partial V}{\partial P}\right)_{T,N_w,N_s} dP + \left(\frac{\partial V}{\partial N_w}\right)_{P,T,N_s} dN_w + \left(\frac{\partial V}{\partial N_s}\right)_{P,T,N_w} dN_s \tag{A7}$$

and, therefore,

$$\left(\frac{\partial V}{\partial N_s}\right)_{P,N_w,\psi} = \left(\frac{\partial V}{\partial N_s}\right)_{P,T,N_w} + \left(\frac{\partial V}{\partial T}\right)_{P,N_w,N_s}\left(\frac{\partial T}{\partial N_s}\right)_{P,N_w,\psi}. \tag{A8}$$

When $\psi=0$, $(\partial V/\partial T)_{P,N_w,N_s}=0$ [see (A1)], hence

$$\left(\frac{\partial V}{\partial N_s}\right)_{P,N_w,\psi=0} = \bar{v}_s \tag{A9}$$

and, at infinite dilution,

$$\lim_{x_s\to 0}\left(\frac{\partial V}{\partial N_s}\right)_{P,N_w,\psi=0} = \bar{v}_s^{\infty}. \tag{A10}$$

Next, we write [see (A4)]

$$N_w\left(\frac{\partial\psi}{\partial V}\right)_{T,N_w,N_s}=\left(\frac{\partial\psi}{\partial 1/\rho_w}\right)_{T,N_w,N_s}=-\rho_w^2\left(\frac{\partial\psi}{\partial\rho_w}\right)_{T,N_w,N_s}. \tag{A11}$$

At infinite dilution,

$$\lim_{x_s\to 0}\left[-\rho_w^2\left(\frac{\partial\psi}{\partial\rho_w}\right)_{T,N_w,N_s}\right]=-\rho_w^2\left(\frac{\partial^2 P}{\partial T\partial\rho_w}\right)^0. \tag{A12}$$

Likewise,

$$\lim_{x_s\to 0}\left(\frac{\partial\psi}{\partial T}\right)_{V,N_w,N_s}=\left(\frac{\partial^2 P}{\partial T^2}\right)^0_{\rho_w}. \tag{A13}$$

Therefore, from (A10), (A12), and (A13), the first group of terms on the right-hand side of (A4) becomes, at infinite dilution,

$$-\left(\frac{\partial V}{\partial N_s}\right)_{P,N_w,\psi}\frac{N_w(\partial\psi/\partial V)_{T,N_w,N_s}}{(\partial\psi/\partial T)_{V,N_w,N_s}}=\rho_w^2\bar{v}_s^{\infty}\frac{(\partial^2 P/\partial T\partial\rho_w)^0}{(\partial^2 P/\partial T^2)^0_{\rho_w}}. \tag{A14}$$

We now consider the numerator of the last term on the right side of (A4),

$$N_w\left(\frac{\partial\psi}{\partial N_s}\right)_{T,V,N_w}=N_w\frac{\partial^2 P}{\partial T\partial N_s}=\frac{N_w^2}{N^2}\frac{\partial^2 P}{\partial T\partial x_s}=\left(\frac{\partial^2 P}{\partial T\partial x_s}\right)^{\infty}, \tag{A15}$$

where the final result is valid at infinite dilution. Finally, substituting (A6), (A14), and (A15) into (A4) we obtain Eq. (14),

$$\left(\frac{\partial T_{\mathrm{MD}}}{\partial x_s}\right)^{\infty}_P=\rho_w^2\bar{v}_s^{\infty}\frac{(\partial^2 P/\partial T\partial\rho_w)^0}{(\partial^2 P/\partial T^2)^0_{\rho_w}}-\frac{(\partial^2 P/\partial T\partial x_s)^{\infty}}{(\partial^2 P/\partial T^2)^0_{\rho_w}}.$$

The only term in the equation of state that depends on the attractive parameters a_{ww} and a_{ss} is $-a\rho^2$ [see Eq. (10)], where $a=x_w^2a_{\mathrm{ww}}+2x_wx_sa_{\mathrm{sw}}+x_s^2a_{\mathrm{ss}}$. It follows that none of the second derivatives of P on the right-hand side of (14) is a function of a_{ss}, as stated in Sec. III.

2. Derivation of Eq. (16)

We first write the identity

$$\bar{v}_s=-VK_T\left(\frac{\partial\mu_s}{\partial V}\right)_{T,N_w,N_s}. \tag{A16}$$

The solute's chemical potential has the form.[4]

$$\mu_s(a_{\mathrm{ss}})-\mu_s(a_{\mathrm{ss}}=0)=-2(\rho_wa_{\mathrm{sw}}+\rho_sa_{\mathrm{ss}}). \tag{A17}$$

Therefore,

$$\left(\frac{\partial\mu_s}{\partial V}\right)_{T,N_w,N_s}-\left(\frac{\partial\mu_s(a_{\mathrm{ss}}=0)}{\partial V}\right)_{T,N_w,N_s}=\frac{2}{V}(\rho_wa_{\mathrm{sw}}+\rho_sa_{\mathrm{ss}}). \tag{A18}$$

From (A16) and (A18) we obtain Eq. (16)

$$\bar{v}_s^{\infty}(\sigma_s,a_{\mathrm{ss}}\neq 0)-\bar{v}_s^{\infty}(\sigma_s,a_{\mathrm{ss}}=0)=-2K_T^0\rho_wa_{\mathrm{sw}}.$$

3. Partial molar volume of a point solute

The chemical potential of a point solute is given by

$$\mu_s=k_BT\ln\rho_s\Lambda_s^3, \tag{A19}$$

where Λ_s is the solute's de Broglie wavelength. Then from Eq. (A16), we obtain, for a point solute,

$$\bar{v}_s=k_BTK_T. \tag{A20}$$

[1] C. Tanford, *The Hydrophobic Effect: Formation of Micelles and Biological Membranes*, 2nd ed. (Wiley, New York, 1980).
[2] W. Kauzmann, Adv. Protein Chem. **14**, 1 (1959).
[3] W. Blokzijl and J. B. F. N. Engberts, Angew. Chem., Int. Ed. Engl. **32**, 1545 (1993).
[4] H. S. Ashbaugh, T. M. Truskett, and P. G. Debenedetti, J. Chem. Phys. **116**, 2907 (2002).
[5] S. Garde and H. S. Ashbaugh, J. Chem. Phys. **115**, 977 (2001).
[6] S. Garde, A. E. García, L. R. Pratt, and G. Hummer, Biophys. Chem. **78**, 21 (1999).
[7] S. Garde, G. Hummer, A. E. García, M. E. Paulaitis, and L. R. Pratt, Phys. Rev. Lett. **77**, 4966 (1996).
[8] G. Hummer, S. Garde, A. E. García, M. E. Paulaitis, and L. R. Pratt, J. Phys. Chem. B **102**, 10469 (1998).
[9] G. Hummer, S. Garde, A. E. García, A. Pohorille, and L. R. Pratt, Proc. Natl. Acad. Sci. U.S.A. **93**, 8951 (1996).
[10] G. Hummer, S. Garde, A. E. García, and L. R. Pratt, Chem. Phys. **258**, 349 (2000).
[11] I. Nezbeda, Fluid Phase Equilib. **170**, 13 (2000).
[12] H. S. Ashbaugh and L. R. Pratt, Rev. Mod. Phys. (in press).
[13] D. Paschek, Phys. Rev. Lett. **94**, 217802 (2005).
[14] P. G. Debenedetti, J. Phys.: Condens. Matter **15**, R1669 (2003).
[15] T. Koop, B. Luo, A. Tsias, and T. Peter, Nature (London) **406**, 611 (2000).
[16] M. B. Baker and M. Baker, Geophys. Res. Lett. **31**, L19102 (2004).
[17] F. B. Salisbury and C. W. Ross, *Plant Physiology*, 4th ed. (Wadsworth, Belmont, 1992).
[18] R. I. S. Haines and S. I. Sandler, J. Chem. Eng. Data **40**, 833 (1995).
[19] T. M. Truskett, P. G. Debenedetti, S. Sastry, and S. Torquato, J. Chem. Phys. **111**, 2647 (1999).
[20] G. Wada, E. Nagao, K. Kawamura, and K. Kinumoto, Bull. Chem. Soc. Jpn. **51**, 1937 (1978).
[21] D. R. Caldwell, Deep-Sea Res. **25**, 175 (1978).
[22] K. Takuizumi and T. Wakabayashi, Bull. Chem. Soc. Jpn. **55**, 2239 (1982).
[23] M. V. Kaulgud and W. K. Pokale, J. Chem. Soc., Faraday Trans. **88**, 997 (1992).
[24] M. V. Kaulgud and W. K. Pokale, J. Chem. Soc., Faraday Trans. **91**, 999 (1995).
[25] A. J. Darnell and J. Greyson, J. Phys. Chem. **72**, 3021 (1968).
[26] J. L. Neal and D. A. I. Goring, J. Phys. Chem. **74**, 658 (1970).
[27] G. Wada and S. Umeda, Bull. Chem. Soc. Jpn. **35**, 646 (1962).
[28] F. Franks and B. Watson, Trans. Faraday Soc. **63**, 329 (1967).
[29] D. D. Macdonald, B. Dolan, and J. B. Hyne, J. Solution Chem. **5**, 405 (1976).
[30] D. D. Macdonald, A. Maclean, and J. B. Hyne, J. Solution Chem. **8**, 97 (1979).
[31] M. V. Kaulgud, J. Chem. Soc., Faraday Trans. **86**, 911 (1990).
[32] M. Oguni and C. A. Angell, J. Chem. Phys. **73**, 1948 (1980).
[33] A. J. Easteal and L. A. Woolf, J. Chem. Thermodyn. **17**, 49 (1985).
[34] C. Xiao, H. Bianchi, and P. R. Tremaine, J. Chem. Thermodyn. **29**, 261 (1997).
[35] K. Tamura, A. Osaki, and Y. Koga, Phys. Chem. Chem. Phys. **1**, 121 (1999).
[36] A. Petek, D. Pecar, and V. Dolecek, Acta Chim. Slov. **48**, 317 (2001).
[37] J. Safarov, S. Heydarov, A. Shahverdiyev, and E. Hassel, J. Chem. Thermodyn. **36**, 541 (2004).